Low Temperature Physics/Fizika Nizkikh Temperatur, 2021, vol. 47, No. 4, pp. 365–377

Low-temperature secondary emission mass spectrometric investigations of a condensed-phase environment of biologically significant compounds

Marina V. Kosevich, Oleg A. Boryak, and Vadim S. Shelkovsky

B. Verkin Institute for Low Temperature Physics and Engineering of the National Academy of Sciences of Ukraine
Kharkiv 61103, Ukraine
E-mail: mvkosevich@ilt.kharkov.ua

Received November 16, 2020, published online February 26, 2021

The main features of the secondary emission mass spectrometry probing of condensed systems containing compounds of biological significance at low temperatures are summarized. The possibilities of distinguishing mass spectra of the solid and liquid phases of simple organic compounds and water as the medium for biomolecules, monitoring of phase transitions and nonequilibrium processes are illustrated. The peculiarities of a model of sputtering of metastable liquids are described. On the basis of the evaluation of these findings, an idea concerning the probable source of relatively large clusters of organic molecules and ions emerging on sputtering of the liquid phase of organic matter condensed on dust grains in space is proposed and discussed.

Keywords: low-temperature secondary emission mass spectrometry, biomolecules, water ice, alcohols, phase transitions.

1. Introduction

Modern mass spectrometry provides much more research opportunities than just mass measurement for the identification of atoms and molecules. Various systems and processes can be modeled under the conditions of mass spectrometric experiments. In particular, a desorption/ionization step required for mass analysis supplies information on interactions of ionizing agents (atoms, ions, nanoparticles, laser irradiation) with the condensed matter. Creating conditions favorable for clustering of molecules and ions allows exploration of noncovalent intermolecular interactions and ion-molecule reactions. Variation of the sample temperature in a wide range permits to study the processes occurring at high or low temperatures.

An original purpose of application of low-temperature (LT) techniques in desorption mass spectrometry was to keep in the condensed state the substances that are gaseous or volatile under ambient conditions. Since mass spectrometric analysis is successfully performed for such compounds in the gaseous state, from the point of view of formal logic, a question may arise why it is necessary to condense these compounds prior to their repeat transfer to the gas phase. As mentioned above, the research interest here goes beyond an ordinary analytical task of identification but is aimed at probing some physical properties of the condensed state of a given compound. Low temperature and pressure, together with ionizing irradiation present in a mass spectrometric setup, are suitable for modeling conditions in space and upper layers of the atmosphere.

As to terminology, two main methods of sputtering or desorpting ions from the condensed state are traditionally named secondary ion mass spectrometry (SIMS) when solid or liquid (liquid SIMS) samples are subjected to irradiation by ions and fast atom bombardment (FAB) when liquid samples are bombarded by neutral atoms.

The history of the development of LT secondary emission mass spectrometry can be found in Refs. 1–8. This work summarizes the general principles of low-temperature studies of systems containing compounds of biological significance in the condensed state [9–18]. The objects of research are not biomolecules *per se*, but the biomolecules in environments occurring in nature or artificially created, such as water, cryoprotector agents, organic solvents, and inorganic components. Modeling of systems composed of these compounds in the low-temperatures range is in demand in research related to cryobiophysics, cryobiology, and problems of organic matter in cosmic space.

Secondary emission mass spectrometric experiments at low temperatures [1–6, 19–22] began long before present-day soft ionization techniques for analysis of biomolecules were developed. At that time, it was believed that the processes

observed at LT SIMS are similar to those occurring under common ambient SIMS of solid objects. In fact, the situation appeared to be more complicated, since the temperatures of various phase transformations of volatile organic compounds and water-containing systems fall into the relatively wide subzero temperature range (accepted in cryobiology as below 273 K). Long-term experience of low-temperature physics research [23] helped to explain the main features of LT FAB/SIMS mass spectra of organic compounds. Let us consider such issues as distinguishing the mass spectra of the solid and liquid phases of simple organic compounds, monitoring phase transitions and non-equilibrium processes, probing the nanostructured surface of frozen water solutions, crystallization of amorphous solid water and a "bubble chamber" model [9] of sputtering liquids under FAB/SIMS conditions. The possibilities provided by LT FAB/SIMS in cryobiophysical and cryobiological research have been demonstrated. An idea of a possible mechanism of transfer of relatively large clusters of organic molecules and ions to the gas phase by sputtering the liquid phase of organic matter condensed on dust grains in space, which provides an additional source of reagents for the prebiotic chemical evolution, is discussed.

2. Methods

A general description of SIMS and FAB methods is given in [24–28]. The LT version of SIMS is usually realized by the insertion of a cryogenic unit for sample cooling into the secondary ion source [19]. This unit is kept at a constant low temperature provided by cryogenic liquids (liquid nitrogen as a rule or helium [29]), cooling, although temperature control of the unit may be provided [21]. An alternative approach is the spontaneous thawing of sample holder being cooled initially in the vapors of liquid nitrogen [7, 30, 31]. In the routine LT FAB/SIMS experiments with water and organic compounds, the lowest temperatures available are usually limited by properties of liquid nitrogen as a cryogenic agent, i.e., 77 K as the temperature of its evaporation.

Two types of experimental setups were used in the experiments. LT FAB experiments were carried out on an MI1201E sector magnetic mass spectrometer ("SELMI", Sumy, Ukraine) equipped with a cryogenic block placed in the secondary ion source [32]. The advantage of the LT ion source design was the ability to the control and measure temperature, which allowed us to obtain temperature dependences of mass spectra both on thawing and freezing (temperature cycling) of samples. Argon atoms with the primary beam energy of 4–5 keV were used as a bombarding agent. LT SIMS experiments were performed using VG-ZAB-SEQ double-focusing mass spectrometer ("Micromass", Manchester, Great Britain). Cs^+ ions with an energy of 30 keV were used. Freezing of liquid samples directly on the sample holder and a spontaneous thawing mode were used. Periodical recording of mass spectra during programmed or a spontaneous warming permits the construction of so-called ion thermograms (analog to chromatograms), i.e., the dependence of the ion current of any ion on time and temperature.

The objects of studies were systems composed of water, organic solvents with antifreeze and cryoprotective properties, such as primary alcohols (methanol, ethanol, propanol, butanol), polyatomic alcohols (ethylene glycol, glycerol), solutions of small biomolecules (amino acids, nitrogen bases) subjected to low temperatures in the 77–273 K range.

3. Manifestations of phase state and phase transitions in the LT FAB/SIMS mass spectra

In the early works on LT secondary emission mass spectrometry, some straightforward predictions concerning the outcome of matter sputtering from the cooled samples were not justified. The first successes with the production of large sets of water clusters $(H_2O)_n^+$ by LT FAB [33–36] and LT SIMS [2, 20, 37] from water ice have raised expectations for sputtering of large hydrated clusters of biomolecules from the frozen aqueous solutions. However, such hydrate clusters have not been obtained, although molecular ions of simple organic compounds have been produced [38–41]. Further, in the relevant LT SIMS investigations [19], a direct correlation of the type of LT mass spectrum of primary alcohol methanol with its reference melting temperature (solid-liquid transition) was not observed.

According to the experimental data [15, 42–47], the LT FAB/SIMS technique is sensitive to changes of the physical state of the samples in the temperatures range of 77–273 K. Knowledge of these features will allow correct interpretation of the obtained experimental data. Let us briefly list the known features of the phase behavior and structure of solid water, water-organic mixtures, and organic solvents, which are essential for understanding of secondary emission process and the resulting mass spectra [7] of samples kept at low temperatures and low pressure (characteristics of a mass spectrometric setup).

The cooling and freezing of macroscopic quantities of liquid water unequivocally leads to the crystalline (polycrystalline) form of the solid. The formation of noncrystalline amorphous solid is prevented by the fact that the rate of homogeneous nucleation of the ice crystals in the liquid water noticeably exceeds the cooling rate of 10^5 K/s required for water amorphization. The formation of layers of so-called amorphous solid water (ASW) is possible only by slow deposition of separate water molecules on a cryogenically cooled substrate below the glass transition temperature of water (136 K) under vacuum conditions. The allowed phase transition of water ice under low-pressure conditions is sublimation. The melting of ice is not achievable in a vacuum, since the temperature-dependent sublimation rates of ice provide complete exhaustion of the sample (of typical size used in mass spectrometric analysis) at a temperature of about (218 ± 5) K [10].

In binary and more complex systems, water does not co-crystallize with the most organic and inorganic compounds. Thus, it is impossible to obtain "amorphous water with homogeneously embedded organic molecules" by ordinary (at a rate of 100–200 K/min) or even "very rapid" (but slower than 10^5 K/s) cooling of aqueous solutions. The exception may be the formation of crystallohydrates, but they are considered as new separate compounds having a crystalline structure. Phase separation takes place on the cooling of water solutions of both inorganic and organic compounds, which is quantitatively described by phase diagram schematically presented in Fig. 1(a). An essential feature of such binary systems is the possibility of the existence of the liquid phase up to the so-called eutectic temperature T_e which may be much lower than the solidification/melting temperature of individual components. This type of diagrams is typical for water mixtures with organic solvents such as alcohols [15]. An important consequence is that when the frozen mixture is thawed, the liquid phase will appear at T_e which is lower than the melting temperature of the pure organic solvent. Another point is that it is problematic to measure concentration dependences for such a binary system using LT FAB/SIMS, since the first portion of the liquid that appears during thawing of the frozen sample will have an eutectic composition independently on the initial ratio of the components.

One should take into account not only equilibrium, but nonequilibrium processes and metastable states of the objects under study [Fig. 1(b)]. It is difficult to obtain supercooled water without special precautions, but some organic solvents are prone to supercooling (which is the basis of cryopreservation in cryobiology). Antifreezes or cryoprotectors can stay liquid at temperatures well below their melting point and solidify in amorphous form. It is also possible to obtain superheated organic liquids [Fig. 1(b)]. The melting points of volatile organic compounds such as alcohols and ethers fall into subzero temperature range. After their melting, the liquid phase can survive in vacuum for a definite time due to a low rate of evaporation (e.g., in the case of glycerol matrix at room temperature). Low rates of homogeneous nucleation permit to avoid spontaneous boiling and to preserve such liquids in a metastable superheated state. This point was essential for the development of the model FAB of liquids [9], described in the Sec. 5.

Frozen samples of dilute water solutions of organic molecules usually have a polycrystalline structure with organic and inorganic solutes displaced into the intercrystalline (eutectic) channels. On the contrary, those organic solvents, which undergo supercooling and amorphization, can retain dissolved biomolecules homogeneously distributed within the amorphous solid.

Taking all these features into account helps to interpret the LT FAB/SIMS data. First, the principal impossibility of producing large hydrate clusters of organic and biomolecules (M) of the $M•(H_2O)_n•H^+$-type from the frozen water solutions is substantiated [7, 8, 13, 43, 46]. The estimates show that the dimensions of the structural elements of the surface of frozen water solutions — ice crystallites (on average 10^{-4} m) and intercrystalline channels (~10^{-6} m) — are larger than the diameter of the spot excited by the impact of a bombarding particle (~10^{-8} m) [7]. As a result, the sputtering of the material proceeds independently from the surface regions of different compositions, and the resulting mass spectrum is a superposition of water clusters sputtered from the ice crystallites and solutes originating from the intercrystalline spaces.

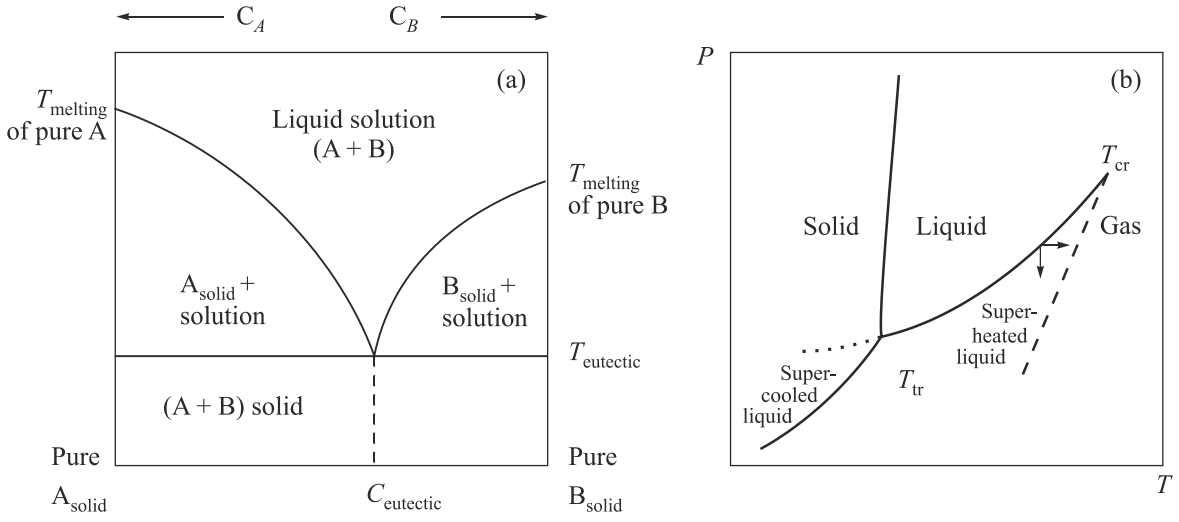

Fig. 1. Typical phase diagrams, essential for interpretation of LT FAB/SIMS data [7, 9]. (a) The phase composition of a binary system (A+B) in dependence of the components ratio and temperature, typical for water solutions of some inorganic and organic compounds. (b) *P–T* dependence, typical for organic solvents: T_{tr} is the triple point, T_{cr} is the critical point; the dotted line shows continuation of the liquid–gas equilibrium line to the metastable area of supercooled liquid; dashed line shows the boundary of the maximal achievable superheating of the liquid.

As to temperature dependences of the LT FAB/SIMS mass spectra of frozen samples of primary alcohols (methanol, ethanol, propanol, butanol), an abrupt change from the low abundant featureless so-called "peak-at-every-mass" or "chemical noise" spectrum to the abundant clean and the reproducible cluster-type spectrum is observed at some temperature on the thawing of the sample, reported both in [19, 31] and our publications [12, 15–18]. We have proved that the temperature of this change correlates with the appearance of the liquid phase in the sample, which may happen below the melting temperature of pure alcohol in the cases of analysis of as-purchased non-dehydrated substances [15]. The eutectic of an alcohol–water binary system, formed even at a very small water content in the initial sample, first melts at T_e [see Fig. 1(a)]. Alcohol–water clusters are sputtered from the liquid of eutectic composition. For example, the temperature of the appearance of the cluster-type spectrum of methanol being about 138 K reported in [19] is close to T_e of methanol–water system, being 135 K, which is 40 K lower than the melting temperature of pure methanol, $T_m \simeq 174$ K. Other constituents of the system may melt (or sublimate) as the temperature rises further. An increase in the rate of evaporation of the liquid with increasing temperature leads to exhaustion of the sample at a predictable temperature.

The directions of liquid alcohols transformations at low temperatures and pressure are similar to those observed at ambient conditions. As an example, let us show how the effect of fractioning for a mixture of liquids with different volatilities (different saturated vapor pressures at a given temperature) can be observed in the low-temperatures range by means of LT SIMS. Figure 2 shows the transformations of the cluster pattern of the mixture of three primary alcohols — methanol (M), ethanol (E), and propanol (P) (the volatility of which decreases in the row) — with increasing temperature. Just after the appearance of the liquid phase during the thawing of the frozen sample, a number of sets of clusters are recorded [Fig. 2(a)], which incorporating the molecules of all components of the $E_n{\bullet}M_m{\bullet}P_k{\bullet}H^+$ system. The cluster sets of ethanol $E_n{\bullet}H^+$ and mixed ethanol-methanol clusters $E_n{\bullet}M{\bullet}H^+$ and $E_n{\bullet}M_2{\bullet}H^+$ dominate the spectrum. Evaporation of methanol with increasing temperature [Fig. 2(b)] is reflected in the suppression of methanol-containing clusters. An increase in the share of propanol remaining in the liquid is reflected in growth of $E_n{\bullet}P{\bullet}H^+$ propanol-containing set. Upon complete evaporation of methanol and partial evaporation of ethanol, propanol-containing $E_n{\bullet}P{\bullet}H^+$ and $E_n{\bullet}P_2{\bullet}H^+$ clusters noticeably increase [Fig. 2(c)]. In another case of a binary methanol-ethanol mixture, a variety of methanol-ethanol mixed clusters recorded after the melting of the sample is gradually substituted by pure ethanol cluster set in the course of methanol evaporation. Interestingly, since ethanol forms an azeotrope with water (i.e., a mixture which cannot be separated by boiling), ethanol–water clusters are observed in LT FAB/SIMS mass spectra of ethanol up to its exhaustion [16–18].

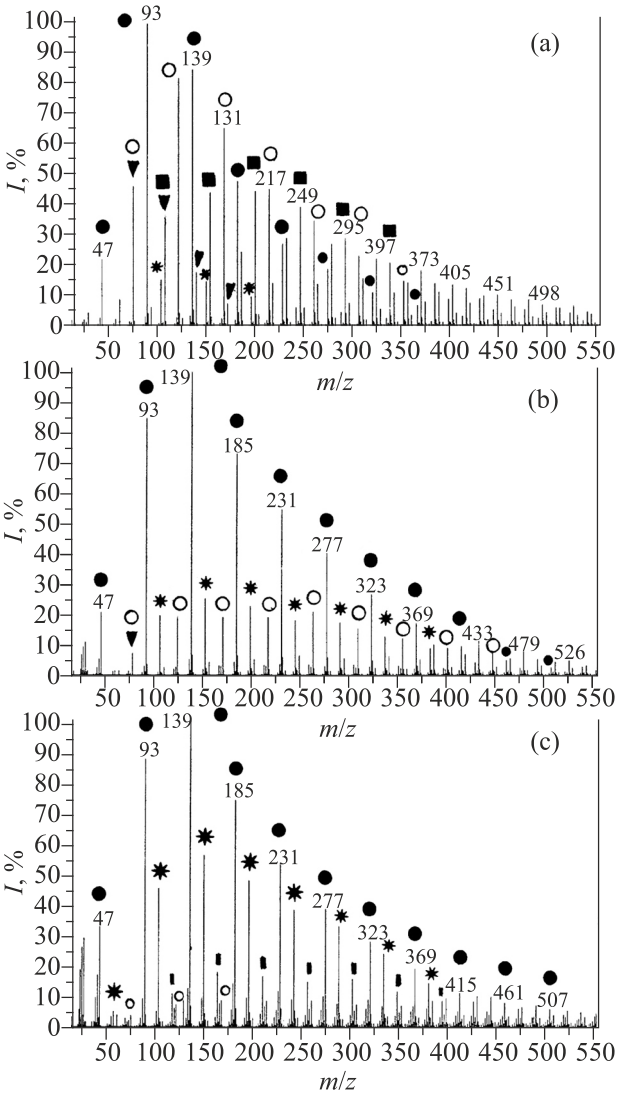

Fig. 2. Transformation of the cluster pattern in the LT SIMS mass spectra of the mixture of three alcohols [methanol:ethanol:propanol (M:E:P)], recorded with gradual increase in the temperature of the liquid sample. The peaks of the cluster sets of various composition ($E_n{\bullet}M_m{\bullet}P_k{\bullet}H^+$) are marked as: $E_n{\bullet}H^+$ (●), $E{\bullet}M_m{\bullet}H^+$ (▼), $E_n{\bullet}M{\bullet}H^+$ (○), $E_n{\bullet}M_2{\bullet}H^+$ (■), $E_n{\bullet}P{\bullet}H^+$ (✱), $E_n{\bullet}P_2{\bullet}H^+$ (▮).

Note that the production of alcohol clusters from the liquid phase was observed with other configurations of mass spectrometric experiments. In works [48, 49], liquid ionization mass spectrometry method was applied to obtain ethanol and mixed ethanol–water clusters from the liquid samples (deposited on the needle tip of chromatography syringe at atmospheric pressure) affected by excited Ar^* atoms (produced by a corona discharge). Abundant sets of multicomponent clusters $(ROH)_m(H_2O)_nH^+$ (where R = CH_3 or C_2H_5) were produced from aqueous solution of ethanol and methanol by the same technique [50]. Positive and negative cluster ions of ethanol were sputtered by 2.0 MeV He^+ ions bombardment of liquid beam target [51].

In the case of polyatomic alcohols prone to supercoolig (ethylene glycol, glycerol), the cluster-type spectrum starts

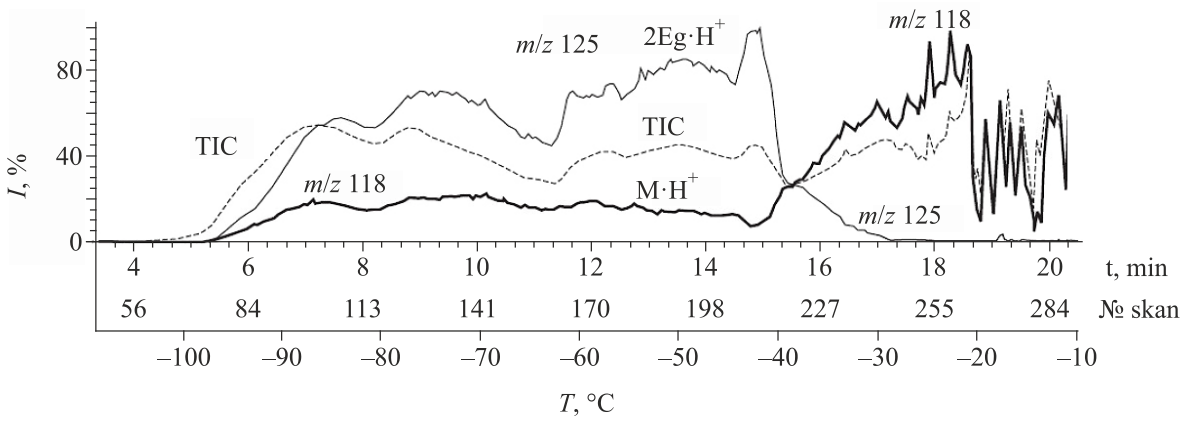

Fig. 3. Ion chromatograms/thermograms recorded by means of LT SIMS during thawing of the frozen sample of amino acid valine (M) solution in ethylene glycol (Eg). Total ion current (TIC) reflects melting of the solid sample, the existence of the liquid phase in a temperature range of approximately 70 °C during about 12 min, and exhaustion of the liquid phase. The signal of valine as protonated molecule M•H^+, *m/z* 118, is present in the spectra during the whole span of the liquid phase existence. (Reproduced from [14] with permission of RSMS).

to emerge upon reaching the glass transition temperature and increases in abundance gradually with decrease in viscosity of the liquid. The time of survival of the liquid phase (which permits to record cluster-type spectra) is predetermined by the rate of evaporation of the liquid at a given temperature and can last from hours and tens of minutes to several seconds. In contrast to aqueous solutions, inorganic and organic solutes dissolved in antifreeze or cryoprotector solvents are trapped in the amorphous solid and are transferred back to the liquid phase on liquefaction of the solid. Due to this, the solutes can be sputtered together with the solvent from the liquid sample during the whole time of the liquid phase existence. Solute-solvent clusters are formed. These features can be illustrated by an example of the LT SIMS study of the solution of amino acid valine in ethylene glycol [14]. In Fig. 3, the ion thermograms of total ion current, ethylene glycol dimer 2Eg•H^+, *m/z* 125, and protonated amino acid M•H^+, *m/z* 118, are shown. It can be seen that the ethylene glycol-related cluster appears at the glass transition temperature, its ion current gradually increases with temperature increase, when viscosity of the sample decreases, and declines when the liquid evaporates. It is noticeable that the signal of amino acid valine M•H^+ is present starting from the melting of the sample and is persist during the whole time span of liquid phase existence. This reflects a positive function of ethylene glycol as an antifreeze (cryoprotector), consisting in preservation of biomolecules in the liquid solution down to low temperatures. In the temperature range of the liquid phase existence, abundant sets of valine clusters solvated by ethylene glycol molecules are recorded both in the positive and negative ion modes. At the temperature of rapid ethylene glycol evaporation, the relative concentration of valine in the remaining liquid increases, which is reflected in noticeable increase in M•H^+ abundance. On drying of the sample over about –20 °C, the solid-state SIMS signal of valine becomes weak and unstable.

Similar results were obtained for some other amino acids in organic solvents with antifreeze properties. In particular, the preservation of the amino acid proline in the liquid phase of ethanol at low temperatures was reported [12].

In terms of the FAB technique, organic solvents can be treated as “liquid matrices” which can be kept in liquid state at low temperatures. For example, volatile solvents suitable for certain compounds were applied in LT FAB studies in the binary pairs methanol-γ-cyclodextrin, dichloromethane–porphyrins [31], toluene–fullerene [52].

Note that similar behavior is observed for those cryoprotector solvents whose saturated vapor pressure values allow them to survive at low pressure at “room” temperature [53]. For example, solvate clusters of biomolecules with polymeric cryoprotectors were obtained for amino acids [54, 55] and nitrogen bases [56] with oxyethylated glycerol oligomers. It may be noted that the whole pool of data accumulated for glycerol can be treated from the point of view of cryoprotector solvents [42], since glycerol is both a popular FAB matrix compound and a popular cryoprotector.

The described features correlate with the useful functions of cryoprotector compounds, consisting in the preservation of biomolecules in the liquid phase to relatively low temperatures and the preservation of the solvation shell of biomolecules [57]. Mass spectrometry permits evaluation of these phenomena at the molecular level. More applications of LT FAB/SIMS to problems of cryobiophysics and cryobiology can be found in our previous reviews [7, 8, 58].

4. Variety of water clusters produced at low temperatures

In the early days of SIMS, a myth has arisen about the insensitivity of the sputtering results to the structure of the solid surface, which is now refuted. Due to lack of experimental information, it was supposed that after the energetic sputtering of some share of material, further events, such

as interaction and clustering of the sputtered species, would be governed by gas-phase chemistry. Later it was revealed that, at least for solid water, the pattern of sputtered clusters has some distinctive features for its dif-ferent forms, crystalline or ASW, in particular, [10]. Moreover, a phenomenon of ASW crystallization was reflected in the peculiar changes in the LT FAB mass spectra [10].

Evaluation of the ice sublimation rates based on the data of investigations conducted earlier [23] shows that for an ice sample of 10 mg on average (usually required for LT mass spectrometric experiments) the rate becomes sufficient for rapid sublimation of the whole sample at (218 ± 5) K [10]. Thus, it is practically impossible to obtain water clusters from pure water ice at temperatures higher this value.

The properties of amorphous and crystalline water and the transition between these two forms are a great interest not only for physics fundamentals [59], but in connection with the modeling of the related processes in outer space [60–62]. Therefore, various complementary experimental techniques are applied to this subject, including temperature-programmed desorption mass spectrometry used to identify the gaseous products released from the ASW layers during their crystallization [63–65] (the process was called the "molecular volcano" due to its abundance [66]).

In our LT FAB experiments, it was shown that the set of protonated water clusters $(H_2O)_n \bullet H^+$ sputtered from ASW layers is characterized by a continuous decrease in the abundance with increasing n (for $n > 1$) [10], while a similar set sputtered from crystalline water ice systematically had a peculiarity of the decrease in abundance of the cluster with $n = 2$ and the increase in abundance for $n = 4$ [44].

The remarkable phenomenon was observed during the heating of the ASW sample [10]: on reaching the temperatures of ASW crystallization, denoted in Ref. 67 as 140–166 K, the sputtering of water clusters was terminated, while the spectra retained the peaks H_3O^+, m/z 19, and $H_2O^{+\bullet}$, m/z 18, correspondings to water monomer. This change was followed by an abundant spectrum of the "peak-at-every-mass" type (Fig. 4), which reflected the release of residual gasses trapped within ASW during its depositin. Such a spectrum can be misinterpreted as a failure of the experiment on water clusters production; in fact, it reflects the real process of "molecular volcano" gases release during the ASW crystallization.

The novelty of our interpretation of the results of LT FAB investigations of ASW crystallization [10] was in account of the phenomenon of so-called explosive crystallization described in Refs. 67–69, which demonstrated that the relaxation of the metastable state of the ASW can be shaken by some external action, which will cause very rapid explosive crystallization. An important feature of this explosive process, often neglected in the routine studies, is the rapid release of the heat of crystallization, which, in contrast to crystallization at equilibrium conditions, can raise the sample surface temperature in 60–80 K. In our LT FAB experiments, accelerated Ar atoms were such an external source of energy able to initiate the crystallization process. As mentioned above, the sputtering of water clusters was terminated at temperatures in the range of the ASW crystallization. It was proposed that all the energy supplied to the sample by bombarding atoms should be spent on the initiating the crystallization process, but not on sputtering the solid. While the sample temperature was kept around 150 K, the thermal spike (in 60–80 K) on its crystallizing surface provided the local surface temperature of ~210–230 K, sufficient for intense ice sublimation. The effect was reflected in the mass spectra by the appearance of molecular ion-radical of water $H_2O^{+\bullet}$, which, as is known, is produced by gas-phase FAB ionization [70]. Note that under the described conditions, the amount of heat required for ice sublimation is not

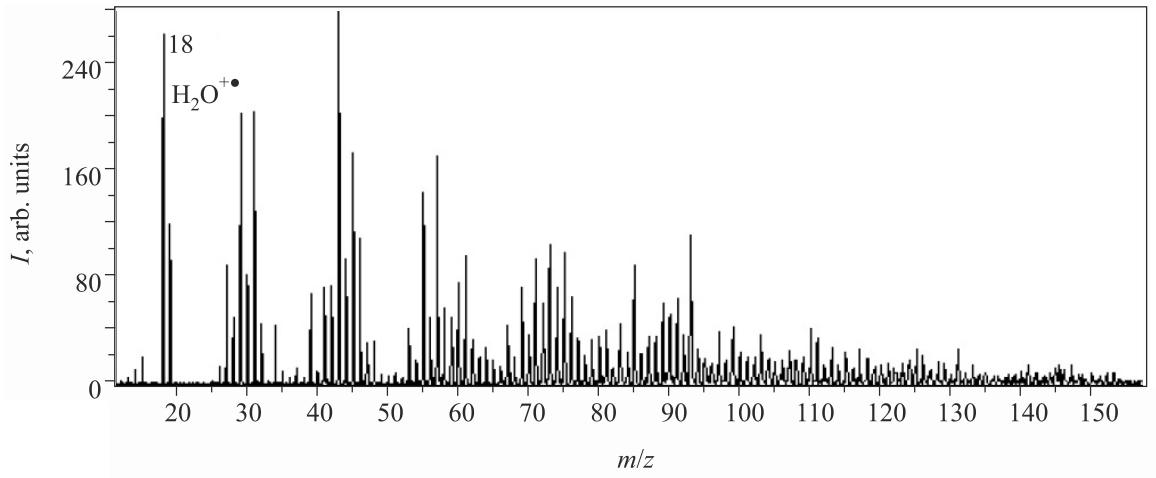

Fig. 4. LT FAB mass spectrum, recorded on warming of ASW sample to the temperature of about 170 K, related to crystallization of ASW. The "peak-at-every-mass" pattern corresponds to volatile compounds trapped within ASW during its deposition and released due to structural rearrangement during the crystallization of the ASW. $H_2O^{+\bullet}$ ion-radical is produced from the sublimating water molecules by the gas-phase FAB mechanism.

supplied by bombarding particles, but is generated within the sample as the heat of ASW crystallization. The self-heating of the surface, along with structural rearrangement, facilitated the release of gases initially trapped within ASW. After the completion of these transformations and the cooling of the surface caused by active sublimation, the regular sputtering of water clusters with a distribution characteristic of crystalline ice (if it remained or initially presented as the substrate) was restored and lasted until the warming of the sample up to the temperature of complete sublimation of the ice sample [(218 ± 5) K].

Consideration of the possibility of active sublimation of water molecules due to "self-heating" of the surface to 60–80 K higher than the underneath substrate in the course of ASW layers explosive crystallization may fill the gap in the estimates of the rates of matter transfer from solid ice mantles of dust grains to the gas phase in model space research. To the best of our knowledge, the contribution of the explosive heat release during the ASW crystallization as a source of local temperature rise sufficient for the noticeable acceleration of ice sublimation was not taken into account in the model experiments on the bombardment of ice by energetic particles. In the framework of the thermal explosion mechanism proposed in [71], the energy consumption of bombarding particles on local heating (thermal spike) of ice was estimated. An additional source of heating was envisaged in exothermic reactions between reactive radical species frozen in ice or exothermic surface reactions [72].

The sensitivity of secondary ion emission to phase transitions in ice was reported for vapor-deposited water ice bombarded by 0.5–1.7 MeV N^{2+} ions in 10–130 K temperature range [73]. A decrease in the total yield of the water cluster ions $(H_2O)_nH_3O^+$ (n up to 30) was observed in the range 38–78 K and was attributed by change of amorphous ice phases from high-density to low-density form [73]. Mixing of residual gaseous organic compounds with amorphous ice was addressed by this technique as well [74]. The features of the water clusters sputtering from ice by various ionizing agents were summarized in Refs. 75, 76.

Another source of water under LT conditions is crystalline hydrates [77]. Correlations of LT FAB/SIMS mass spectra with phase diagrams of binary systems composed of water and some inorganic compounds are presented in [44–47, 58, 78–81]. Let us list the main features of water-containing clusters production. The water-acid H_2O–HCl system [78] is characterized by the existence of a number of crystalline hydrates $HCl•nH_2O$ (n = 1, 2, 3, 6). A set of protonated water clusters $(H_2O)_n•H^+$ (n = 1–12), sputtered by FAB from the frozen HCl aqueous solutions, has abundances noticeably higher than those in the set produced from pure water ice, which is explained by the proton H^+ origination from the acid molecules in the crystalline hydrates.

In the H_2O–HNO_3 system [79], mono and trihydrates $HNO_3•nH_2O$ can be formed on cooling. In the LT FAB mass spectra of the frozen system, a set of water clusters with monotonously decreasing abundance is present along with a number of bell-shape sets of hydrate clusters with various combinations of the components: $(H_2O)_n•NO^+$, $(H_2O)_n•NO_2^+$, $(HNO_3)_m•(H_2O)_n•H^+$ (m = 1–6, n = 1–15). The formation of the same type of crystalline hydrate on freezing of the HNO_3 solution independently on its initial concentration (in some range defined by the phase diagram) hinders determination of the concentration dependences based on of LT FAB mass spectra [82].

The most interesting conclusion, derived from the LT FAB study of the H_2O–HNO_3 system [79], relates to the interpretation of the results of *in situ* mass spectrometric recording of cluster composition of the upper layers of atmosphere near the noctilucent clouds [83]. One of the recorded there bell-shaped set of clusters was attributed to water. However, the pattern of the supposed set $(H_2O)_n•H^+$ was quite unusual, since the n values were in the range of 9–20 only and the maximum of the "bell" was at n = 15, 16, which was never observed for neat water ice. Our data for the H_2O–HNO_3 system [79] show that the masses and distribution in this set may correspond to $(HNO_3)_2•(H_2O)_n•H^+$ (n = 6–12) series, originating from the frozen nitric acid trihydrate. This allowed us to suggest the presence of nitric acid in the composition of the noctilucent clouds [79].

The low vapor pressure of sulfuric acid H_2SO_4 permits to study it by means of FAB at room temperature and to obtain hydrate clusters reported in [84]; they were also obtained at low temperatures [85–87].

Hydrate clusters were observed in the LT FAB mass spectra of water-inorganic salts systems in the case of the formation of crystalline hydrates of salts in the low-temperature range. The formation of $NaCl•2H_2O$ crystalline hydrate in H_2O–NaCl system was reflected in sputtering of $(H_2O)_n•Na^+$ and $(H_2O)_n•NaCl•Na^+$ clusters [44, 45]. The observation of similar types of clusters for D_2O–NaCl system allowed us to suggest the existence of NaCl crystalline hydrate with heavy water [46], which was not reported earlier in the literature. Hydrate clusters of salt cations were recorded in LT FAB mass spectra of frozen water solutions of a number of divalent metal salts $MgCl_2$, $CaCl_2$, $MnCl_2$, $CuCl_2$, $ZnCl_2$, $BaCl_2$ [80, 81], the phase diagrams of which indicate the formation of crystalline hydrates. By now, we failed to find crystalline hydrates of organic compounds, which can serve as a source of hydrate clusters under LT FAB.

5. "Bubble chamber" model of FAB of liquids

Analysis of the FAB/SIMS mass spectral information obtained in the temperature range widened to low temperatures, in particular, allowed us to formulate a model of the processes occurring under the conditions of energetic particles bombardment of liquids, called the "bubble chamber" model [9].

The starting points for the development of this model were as follows. First, the qualitative difference between

secondary emission mass spectra obtained for solid and liquid phases of the same compound was proved. Second, on the example of alcohols, it was shown that the pattern of clusters sputtered from the liquid does not depend on the type, energy, and charge state of bombarding particles and is qualitatively the same, e.g., for the bombardment of 4–5 keV argon atoms [16], 8 keV Ar^+ [19], 6–8 keV Xe [6, 31], and 30 keV Cs^+ ions [17, 18], as well as 2.0 MeV He^+ ions applied in liquid-beam technique [51]. This may mean that all bombarding agents of any type and energy initiate the same process in the liquid, which gives the same result. Third, our estimates of the pressure-temperature dependences of the organic compounds under study [9, 11] and the evaluation of their phase state have shown that the liquid phase of all studied alcohols and diethyl ether appear in the superheated state under vacuum conditions. This is the crucial point for our model, since it is known that an external energetic effect on the metastable superheated liquid initiates its boiling, that is, the formation of the gas phase in the form of growing bubbles. This property of superheated liquids was employed in the bubble chamber devices which, along with Wilson chambers utilizing oversaturated vapor, were designed in the early days of nuclear physics and space research for the recording of ionizing radiation and cosmic rays. The effect was the same for all types of the recorded energetic particles and consisted in the initiation of the phase transition in the metastable medium visualized by a trace of bubbles along the particle track.

We have proposed that a similar process of boiling is initiated by bombarding particles under FAB and liquid SIMS conditions [9]. In such a case, the formation and burst of microscopic bubbles grown near the surface of the liquid sample, result in the release of gas, clusters, and tiny droplets of the analyte. The role of bombarding agents, independently of their type and energy, is the initiation of boiling of the superheated liquid in the particle impact zone. Further events are determined by the properties of the liquid *per se*. Note that the boiling of alcohols proceeds at low temperatures, i.e., the temperature of the whole sample remains low. This process may be called the "nonthermal" mechanism of the matter transfer from the liquid to the gas phase. Such a process is allowed only for the liquid phase and, consequently, does not realized in the solid phase of the same compound. Thus, the sputtering of matter from the solid organic sample at temperatures only a several degrees below their melting point will proceed via common solid phase SIMS and, as a rule, will result in comparatively low-abundant products of direct sputtering and thermal damage.

To verify this model, we have performed the LT SIMS experiment for the liquid utilized in real bubble chambers, i.e., diethyl ether [11]. Preliminary calculations have shown that the liquid phase of this highly volatile compound will survive under low-pressure conditions for a several seconds only. Indeed, about one minute after the melting of the frozen diethyl ether sample was available for very rapid recording of the cluster-type spectra characteristic of the liquid phase.

Thus, the "bubble chamber" model permits to explain abundant production of various ionized species on the sputtering of liquids under FAB/SIMS conditions.

6. Miscellaneous

For completeness, we briefly list some other ionization/desorption techniques applied to the study of frozen water and organic samples.

In the course of development of laser desorption/ionization (LDI) techniques suitable for biomolecules analysis crowned by matrix-assisted LDI (MALDI), water ice was tested as a possible matrix [88–99]. The main difficulties in solving this task were the low efficiency of ice-containing samples sputtering by UV lasers and low efficiency of ionization of biomolecules by IR lasers. Combinations of the sample material (ice) desorption by IR laser followed by ionization of the desorbed material by UV laser [100, 101], single [88] or multiphoton [92] ionization were developed. Mass spectra of biopolymers, such as polypeptides and proteins [91, 93, 94, 96], nucleic acids [89, 90], polysaccharides glycosaminoglycans [97], carbohydrates, and glycolipids [95], were obtained by LDI from frozen water solutions.

IR optical parametric oscillator laser resonant desorption technique permitted the production of large water clusters $H_3O^+(H_2O)_n$ ($n \approx 100$) from ice at 90 K [98] and hydrate clusters of organic and biomolecules [99]. In particular, clusters of tryptophan amino acid with up to 20 water molecules were generated from the frozen water solution (at 90 K) [99], that differentiates the LDI results from those of LT FAB [7, 43, 46]. This effect is predetermined by the differences in sample sputtering by laser irradiation and particle bombardment and is in agreement with the model of sputtering, which accounts the structure of the frozen water solutions formed due to phase separation during freezing [7]. Namely, the diameter of a spot excited by a single bombarding particle being 10^{-8} m provides an independent sputtering of water clusters from ice crystallites (10^{-4} m) and ions of the solute expelled to the intercrystallite channels (~10^{-6} m). At the same time, the spot diameter of ~$3\cdot10^{-4}$ m affected by a laser impulse [99] is sufficient for material desorption from a number of the surface structural elements simultaneously resulting in the mixing and subsequent clustering of water and analyte molecules in the gas phase.

Water ice is also applied as a matrix in emerging imaging techniques including LDI for proteins imaging [102], IR-MALDESI (MALDI combined with electrospray ionization) for biological tissues imaging [103, 104], and *in vivo* water-assisted LDI (WALDI) [105].

Freezing of biological materials is used in imaging techniques based on SIMS combined with time-of-flight (TOF) mass analyzers [106, 107], in particular, cryo-TOF-SIMS [108]. Harnessing of novel "cluster or polyatomic

ion beams primary ion sources" [109] permits molecular depth profiling and 3-dimensional rendering of the frozen objects [110].

The hazard of the plasma desorption mass spectrometry (PDMS) method, which utilizes bombardment by fission products of ^{252}Cf, developed at the end of the last century, caused its rapid substitution by other ionization techniques in the biomedical research area. However, the possibility of affecting a sample by MeV particles secured its successful application in basic physics research, for example, the use ^{252}Cf-PDMS-TOF applications to MeV bombardment of space-related ices, including reports on 65-MeV heavy ion bombardment of methanol frozen at 55 K [111] and formic acid [112], which is in relevant for the solid state astrochemistry.

In connection with studies of frozen water, it is worth to mention investigations of practical importance aimed at the determination of contaminants and ecological pollutants in natural snows of various origin, performed by advanced two-dimensional gas chromatography with high-resolution mass spectrometry [113–115] and FT-ICR [116] techniques.

7. Implications of LT FAB/SIMS data for space science

Based on the LT FAB/SIMS information, we enunciate and substantiate an idea concerning the involvement of the liquid phase of simple organic compounds sputtered by energetic particles as a lacking source of reactive species for chemical transformations considered in the framework of astrochemistry and astrophysics.

Chemical evolution in the Universe, resulting in the emergence of complex organic molecules and further biomolecules, is of interest to multidisciplinary scientists [117–120] and stimulates numerous experiments [121, 122], including mass spectrometric approaches [123–127]. The low-pressure and low-temperature conditions created in mass spectrometric experiments, together with the irradiation of samples by energetic particles in the frame of secondary emission techniques, are suitable for imitating the space environment.

The initial concepts of the outer space as a cold and airless medium justified model experiments with objects in the solid phase which is characteristic for simple organic compounds and water under such conditions. Various experiments have provided precious information on the chemical transformations occurring in the ices composed of water and organic molecules adsorbed at the surface of inorganic dust grains under the effect of their collisions with energetic particles, and on solid-gas transitions of the reactions' products [117–119]. However, a number of essential issues within this problem still wait for their clarification. First, the quantitative and qualitative composition of the gas-phase species sputtered from the solid ice mantles of dust grains, determined in such experiments, is insufficient to match to the quantity and variety of gas-phase reactive species detected in the corresponding space regions. Second, the search continues for the so-called nonthermal mechanisms of the matter transfer from the condensed to the gas phase as an alternative to thermal desorption. To the best of our knowledge, the liquid phase of the organic compounds in question and liquid–gas transitions were not considered in this context.

In the proposed model, we are trying to reproduce only one essential "chain link" of condensed phase–gas phase transition, which is missing now. We proceed from the assumption that some amount of organic compounds has already formed and exists in the adsorbed state on the surface of interstellar dust grains or at the particles in the comet tails. The main events in our "chain link" are as follows:

(i) The liquid phase of simple organic compounds present in the mantle of dust grains can emerge when such grains get into the zone with temperature and pressure parameters required for the existence of the liquid phase. The undisturbed liquid phase can survive in a definite low-temperatures range under vacuum conditions being in the superheated state.

(ii) The impact of an energetic particle of any kind on such a metastable liquid initiates its explosive boiling, i.e., the formation and burst of gas bubbles described in our "bubble chamber model" for FAB/SIMS of liquids [9]. The boiling at a given low temperature agrees with the preconditions of the "nonthermal" mechanism.

(iii) As shown earlier, the amount of matter transferred to the gas phase from the liquid by means of particle bombardment is one-two orders of magnitude larger than the amount sputtered from the solid phase of the same compound. This solves the above-mentioned problem concerning the quantity of organic-related species in the gas phase in space.

(iv) As to qualitative composition, a plethora of neutrals, positively and negatively charged ions, radical cations and anions, fragments, and cluster ions built of up to several tens of molecules are transferred from the liquid to the gas phase. This solves the problem of the origin of some types of relatively large reactive species, emitted to the gas phase, which cannot be produced by destructive sputtering of solids.

(v) Water may be present in the melted eutectic of the water-organic systems. Mixed water-containing clusters are released from the liquids of eutectic composition. Small biomolecules, if present, are incorporated into the liquid phase created, e.g., by alcohols, and are sputtered within the solvate clusters.

Further involvement of the sputtered species in chemical reactions is not predetermined by the proposed model but depends on the characteristics of the surrounding medium. The sputtered particles can either participate in the gas-phase transformations and ion-molecule reactions, or be adsorbed at the neighboring cold surfaces providing a renovated composition of the adsorbed films. Note that while liquid water is required for life processes, the ordinary chemical reaction required for chemical synthesis can proceed in organic solvents.

All the data accumulated in LT FAB and liquid SIMS studies of organic liquids and their mixtures with water and small biomolecules provides "ready-made" sets of reactive species that may be applied in theoretical modeling of the feasible reactions in space. An example of such species can be the constituents of the LT SIMS mass spectra of the primary alcohols mixture presented in Fig. 3 and Refs. 16, 18. Positively and negatively charged protonated and deprotonated clusters $[M_n + H]^+$ and $[M_n - H]^-$ (M is for any alcohol molecule, *n* up to several tens) make the main contribution. Products of fragmentation of excited clusters $[M_n + H - H_2O]^+$, $[M_n + H - X]^+$, $[M_n - X]^-$ (where X is any functional group) are recorded. It is known that M_n neutrals must also be abundantly produced, but they are "invisible" for a given technique. In the case of organic-water-containing systems (eutectic, azeotropes), hydrate clusters $[M_n + H_2O_m + H]^+$, $[M_n + H_2O_m - H]^-$ are transferred to the gas phase [17, 18]. Other organic molecules and metal ions that may get into the melted solvent may be transferred to the gas phase together with the sputtered solvent. Formaldehyde aldehyde deserves special attention, since it produces large sets of polymerization products and hydrates [8, 46]. Here we do not touch one more special issue concerning the irradiation damage products generated in the liquid through energetic particle impact [128, 129].

A natural question arises about the occurrence in the outer space of temperature sufficient for melting of organic compounds adsorbed on dust grains. The estimates of the temperatures in various regions of the Universe available in reviews [117–119] indicate the existence of suitable conditions. In particular, it was established that the surface temperatures of the ice-dust particle in the comets tails when the comets travel near stars can reach 170 K and even 220 K [130]. The estimates of temperatures characteristic of various phases of space evolution are accepted: 10 K inherent to the cold phase undergo rise to ~100 K during the warm-up phase and reach 200–300 K during the hot core phase [118, 131]. Dust grains may be subjected to temperature rise in the event of their entering the upper layers of the planets atmosphere, where the pressure is still low and there is ionizing radiation.

Thus, the explosive boiling of the superheated liquid phase of simple organic compounds, initiated by energetic particle bombardment in the low-temperature range, may comprise the sought-for nonthermal mechanism of the condensed phase–gas phase transition. As a result, there was an abundant release of ions and clusters, the composition of which has already established in the framework of LT FAB/SIMS experiments.

Conclusions

The application of low-temperature techniques in secondary emission mass spectrometry permits to investigate physical transformations in the samples of water, organic solvents, and their multicomponent mixtures with biomolecules. The characteristic patterns of LT FAB/SIMS mass spectra reflect the physical state of the samples and correlate with phase transitions which occur in the range from ambient to liquid nitrogen temperatures. The impact of bombarding particles initiates a phase transition allowed by a phase diagram of the probed system at a given temperature and pressure. Most interesting is the case of metastable states of the systems: particle bombardment initiates explosive crystallization of the amorphous solid water and explosive boiling of the superheated liquids. The process of gas-phase bubbles formation in the liquid organic, being in the superheated state at low temperatures, similar to that utilized in the bubble chambers, comprise a possible mechanism of sample sputtering accompanied by abundant cluster ion formation. It is important that the temperature of the liquid remains low during such an explosive boiling process.

Effects of interest for cryobiophysics and cryobiology can be observed under LT FAB/SIMS conditions. The absence of production of hydrate clusters of small biomolecules from frozen water solution reflects crystallization of ice, phase separation, and dehydration of the biomolecules, while abundant production of solvate clusters of biomolecules from the liquid phase of solvents possessing antifreeze properties reflects the positive function of cryoprotectors.

Analysis of the up-to-date data on the temperature of various objects in space permits to distinguish a circle of conditions analog to those created in LT FAB/SIMS experiments. These conditions enable the existence of the liquid phase of simple organic compounds in predictable temperature ranges. This information allowed us to propose an idea concerning the additional source of reagents for prebiotic chemical evolution in space, simulated by LT FAB/SIMS. Namely, positively and negatively charged clusters, radical-ions, fragment ions, and water-containing clusters are generated from the liquid phase of the organic compounds on energetic particles impact with abundances at least two orders of magnitude higher than the abundances of species sputtered from the solid phase. It is also necessary to take into account the initiation of explosive ASW crystallization by particle bombardment and the active sublimation of water molecules due to local heating of the surface by the heat generated in the course of crystallization. These LT FAB/SIMS observations help to fill a gap in model astrophysical and astrochemical research formulated as a shortage of knowledge on so-called nonthermal desorption mechanisms leading to the transfer of preformed organic from solid grains to the gas phase in space.

Acknowledgments

The research was supported by the Grant No. 0120U100157 of the National Academy of Sciences of Ukraine. The authors are grateful to Professor Karoly Vekey and Dr. Agnes Gomory for long-term cooperation in LT SIMS research.

1. G. D. Tantsyrev and E. N. Nikolaev, *Pis'ma Zh. Eksp.Teor. Fiz.* **13**, 473 (1971) (in Russian) [*JETP Lett.* **13**, 337 (1971)].
2. G. M. Lancaster, F. Honda, Y. Fukuda, and J. W. Rabalais, *J. Amer. Chem. Soc.* **101**, 1951 (1979).
3. R. G. Orth, H. T. Jonkman, and J. Michl, *J. Amer. Chem Soc.* **103**, 1564 (1981).
4. G. D. Tantsyrev, *Int. J. Mass Spectrom. Ion Phys.* **49**, 223 (1983).
5. J. Michl, *Int. J. Mass Spectrom. Ion Phys.* **53**, 255 (1983).
6. J. Sunner, M. G. Ikonomou, and P. Kebarle, *Int. J. Mass Spectrom. Ion Proc.* **82**, 221 (1988).
7. M. V. Kosevich, *Eur. Mass Spectrom.* **4**, 251 (1998).
8. Yu. P. Blagoi, G. G. Sheina, A. Yu. Ivanov, E. D. Radchenko, M. V. Kosevich, V. S. Shelkovsky, O. A. Boryak, and Yu. V. Rubin, *Fiz. Nizk. Temp.* **25**, 1003 (1999) [*Low Temp. Phys.* **25**, 747 (1999)].
9. M. V. Kosevich, V. S. Shelkovsky, O. A. Boryak, and V. V. Orlov, *Rapid Commun. Mass Spectrom.* **17**, 1781 (2003).
10. M. V. Kosevich, O. A. Boryak, V. S. Shelkovsky, and V. V. Orlov, *Fiz. Nizk. Temp.* **29**, 1061 (2003) [*Low Temp. Phys.* **29**, 805 (2003)].
11. M. V. Kosevich, V. S. Shelkovsky, O. A. Boryak, A. Gomory, P. D. Vegh, and K. Vekey, *J. Mass Spectrom.* **38**, 517 (2003).
12. O. A. Boryak, M. V. Kosevich, and V. S. Shelkovsky, *Proc. Kharkov State Univ., Biophysical Bulletin.* **488**, 44 (2000).
13. M. V. Kosevich, O. A. Boryak, V. S. Shelkovsky, V. V. Orlov, V. V. Chagovets, V. A. Karachevtsev, and Yu. P. Blagoi, *Proc. Kharkov State Univ., Biophysical Bulletin.* **593**, 29 (2003).
14. M. V. Kosevich, V. G. Zobnina, O. A. Boryak, V. S. Shelkovsky, A. Gomory, and K. Vekey, *Mass-spektrometria* **3**, 33 (2006) (in Russian).
15. M. V. Kosevich, *Europ. Mass Spectrom.* **3**, 320 (1997).
16. O. A. Boryak, M. V. Kosevich, and V. S. Shelkovsky, *Int. J. Mass Spectrom. Ion Proc.* **163**, 177 (1997).
17. M. V. Kosevich, G. Czira, O. A. Boryak, V. S. Shelkovsky, and K. Vekey, *Rapid Commun. Mass Spectrom.* **11**, 1411 (1997).
18. M. V. Kosevich, G. Czira, O. A. Boryak, V. S. Shelkovsky, and K. Vekey, *J. Mass Spectrom.* **33**, 843 (1998).
19. R. N. Katz, T. Chaudhary, and F. H. Field, *J. Amer. Chem. Soc.* **108**, 3897 (1986).
20. R. N. Katz, T. Chaudhary, and F. H. Field, *Int. J. Mass Spectrom. Ion Proc.* **78**, 85 (1987).
21. K. Heckles, R. A. W. Johnstone, and A. H. Wilby, *Tetrahedron Lett.* **28**, 103 (1987).
22. Yu.-C. Chen, H. L. Chei, and J. Shiea, *J. Mass Spectrom.* **31**, 464 (1996).
23. B. I. Verkin, V. F. Getmanets, and R. S. Mikhalchenko, *Thermophysics of Low-Temperature Sublimational Cooling*, Naukova Dumka, Kiev (1980) (in Russian).
24. V. Cherepin, *Secondary Ion Mass Spectroscopy of Solid Surfaces*, Science Press, Utrecht (1987).
25. A. Benninghoven, F. G. Rudenauer, and H. W. Werner, *Secondary Ion Mass Spectrometry: Basic Concepts, Instrumental Aspects, Applications and Trends*, Wiley, New York (1987).
26. A. Benninghoven, *Int. J. Mass Spectrom. Ion Phys.* **46**, 459 (1983).
27. J. Sunner, *Org. Mass Spectrom.* **28**, 805 (1993).
28. J. H. Gross, *Mass Spectrometry*, Springer, Cham (2017).
29. R. G. Orth, H. T. Jonkman, and J. Michl, *Int. J. Mass Spectrom. Ion Phys.* **43**, 41 (1982).
30. G. D. Tantsyrev and G. B. Pronchev, *Prib. Tekh. Eksp.* **3**, 180 (1995) (in Russian).
31. J. H. Gross, *Rapid Commun. Mass Spectrom.* **12**, 1833 (1998).
32. O. A. Boryak, M. V. Kosevich, and V. S. Shelkovsky, *Prib. Tekh. Eksp.* **6**, 176 (1993) (in Russian).
33. G. D. Tantsyrev and E. N. Nikolaev, *Dok. Akad. Nauk SSSR* **206**, 151 (1972) (in Russian).
34. E. N. Nikolaev and G. D. Tantsyrev, *Zh. Tekh. Fiz.* **45**, 400 (1975) (in Russian).
35. E. N. Nikolaev, G. D. Tantsyrev, and V. A. Saraev, *Zh. Tekh. Fiz.* **46**, 2184 (1976) (in Russian).
36. E. N. Nikolaev and G. D. Tantsyrev, *Khim. Vys. Energ.* **12**, 301 (1978) (in Russian).
37. T. Matsuo, T. Tonuma, H. Kumagai, H. Shibata, and H. Tawara, *J. Chem. Phys.* **101**, 5356 (1994).
38. G. D. Tantsyrev and G. Yu. Lyapin, *Zh. Anal. Khim.* **46**, 1767 (1991) (in Russian).
39. I. A. Malyarova and G. D. Tantsyrev, *Zh. Anal. Khim.* **46**, 1819 (1991) (in Russian).
40. G. B. Pronchev and G. D. Tantsyrev, *Khim. Fiz.* **14**, 44 (1995) (in Russian).
41. G. D. Tantsyrev and G. B. Pronchev, *J. Trace Microprobe Tech.* **17**, 49 (1999).
42. O. A. Boryak, M. V. Kosevich, V. S. Shelkovsky, and Yu. P. Blagoy, *Rapid Commun. Mass Spectrom.* **9**, 978 (1995).
43. O. A. Boryak, M. V. Kosevich, V. S. Shelkovsky, and Yu. P. Blagoy, *Rapid Commun. Mass Spectrom.* **10**, 197 (1996).
44. O. A. Boryak, I. O. Stepanov, M. V. Kosevich, V. S. Shelkovsky, V. V. Orlov, and Yu. P. Blagoy, *Eur. Mass Spectrom.* **2**, 329 (1996).
45. M. V. Kosevich, O. A. Boryak, I. O. Stepanov, and V. S. Shelkovsky, *Eur. Mass Spectrom.* **3**, 11 (1997).
46. M. V. Kosevich, O. A. Boryak, V. S. Shelkovsky, and P. J. Derrick, *Eur. Mass Spectrom.* **4**, 31 (1998).
47. M. V. Kosevich, O. A. Boryak, and V. S. Shelkovsky, *Eur. J. Mass Spectrom.* **8**, 157 (2002).
48. M. Tsuchiya, Y. Li, J. Shirasaka, and T. Kaneko, *Chem. Lett.* **25**, 229 (1996).
49. M. Tsuchiya, H. Fukaya, and Y. Shida, *Mass Spectrom.* **2**, A0015 (2013).
50. M. Tsuchiya, Y. Shida, K. Kobayashi, O. Taniguchi, and S. Okouchi, *Int. J. Mass Spectrom.* **235**, 229 (2004).
51. M. Kaneda, M. Shimizu, T. Hayakawa, Y. Iriki, H. Tsuchida, and A. Itoh, *J. Chem. Phys.* **132**, 144502 (2010).
52. J. H. Gross, S. Giesa, and W. Krätschmer, *Rapid Commun. Mass Spectrom.* **13**, 815 (1999).
53. M. V. Kosevich, V. G. Zobnina, E. N. Zhyvotova, I. V. Shmygol', O. A. Boryak, V. V. Chagovets, V. V. Chekanova, A. V. Zinchenko, V. A. Pokrovsky, and A. Gomory, *Mass-spektrometria* **6**, 7 (2009) (in Russian).

54. V. G. Zobnina, O. A. Boryak, M. V. Kosevich, V. V. Chagovets, V. V. Orlov, V. V. Snegir, V. A. Pokrovsky, E. N. Zhyvotova, A. V. Zinchenko, and A. Gomory, *Biofiz. Visn.* **22**, 103 (2009) (in Russian).
55. M. V. Kosevich, V. G. Zobnina, O. A. Boryak, V. V. Chagovets, and A. V. Zinchenko, *Probl. Kriobiol*. **22**, 327 (2012) (in Russian).
56. V. G. Zobnina, V. V. Chagovets, O. A. Boryak, and M. V. Kosevich, *Mass-spectrometria* **11**, 97 (2014) (in Russian) [*J. Anal. Chem.* **70**, 1533 (2015)].
57. *Water — A Comprehensive Treatise*, *Water and Aqueous Solutions at Subzero Temperatures*, F. Franks (ed.), Vol. 7, Plenum Press, New York (1982).
58. M. V. Kosevich, V. S. Shelkovsky, and O. A. Boryak, in: *Secondary Ion Mass Spectrometry*: *SIMS XII*, A. Benninghoven, P. Bertrand, H. N. Migeon, and H. W. Werner (eds.), Elsevier, Amsterdam (2000).
59. V. F. Petrenko and R. W. Whitworth, *Physics of Ice*, Oxford University Press, New York (1999).
60. P. Jenniskens and D. F. Blake, *Astrophys. J.* **473**, 1104 (1996).
61. R. Martín-Doménech, G. M. Muñoz Caro, J. Bueno, and F. Goesmann, *Astron. Astrophys.* **564**, A8 (2014).
62. E. F. van Dishoeck, *Faraday Discuss.* **168**, 9 (2014).
63. R. A. May, R. S. Smith, and B. D. Kay, *J. Phys. Chem. Lett.* 3, 327 (2012).
64. R. A. May, R. S. Smith, and B. D. Kay, *J. Chem. Phys.* **138**, 104501 (2013).
65. R. Souda, *Chem. Phys. Lett.* **645**, 27 (2016).
66. R. S. Smith, C. Huang, E. K. L. Wong, and B. D. Kay, *Phys. Rev. Lett.* **79**, 909 (1997).
67. V. P. Scripov and V. P. Koverda, *Spontaneous Crystallization of Supercooled Liquids*, Nauka, Moscow (1984) (in Russian).
68. V. P. Koverda, V. P. Skripov, and N. M. Bogdanov, *Dokl. Akad. Nauk SSSR* **212**, 1375 (1973) (in Russian).
69. V. P. Skripov, E. N. Sinitsyn, P. A. Pavlov, G. N. Muratov, N. V. Bulanov, and V. G. Baidakov, *Thermophysical Properties of Liquids in a Metastable State*, Atomizdat, Moscow (1980) (in Russian).
70. M. Takayama, *Int. J. Mass Spectrom. Ion Proc.* 152, 1 (1996).
71. A. V. Ivlev, T. B. Röcker, A. Vasyunin, and P. Caselli, *Astrophys. J.* **805**, 59 (2015).
72. R. T. Garrod, V. Wakelam, and E. Herbst, *A&A* **467**, 1103 (2007)
73. A. L. F. de Barros L. S. Farenzena, D. P. P. Andrade, E. F. da Silveira, and K. Wien, *J. Phys. Chem. C* **115**, 12005 (2011).
74. A. L. F. de Barros, E. F. da Silveira, L. S. Farenzena, and K. Wien, *J. Surf. Invest.: X-Ray, Synchrotron Neutron Tech.* **7**, 1225 (2013).
75. R. A. Baragiola, R. A. Vidal, W. Svendsen, J. Schou, M. Shi, D. A. Bahr, and C. L. Atteberry, *Nucl. Instrum. Methods Phys. Res., Sect. B* **209**, 294 (2003).
76. X. A. Conlan, J. S. Fletcher, N. P. Lockyer, and J. C. Vickerman, *J. Phys. Chem. C* **114**, 5468 (2010).
77. *Water — A Comprehensive Treatise, Water in Crystalline Hydrates. Aqueous Solutions of Simple Nonelectrolytes*, F. Franks (ed.), Vol. 2, Plenum Press, New York (1973).
78. O. A. Boryak, M. V. Kosevich, I. O. Stepanov, and V. S. Shelkovsky, *Int. J. Mass Spectrom.* **189**, L1 (1999).
79. M. V. Kosevich, O. A. Boryak, V. A. Pashinskaya, and V. S. Shelkovsky, *J. Mass Spectrom.* **34**, 1303 (1999).
80. O. A. Boryak, M. V. Kosevich, V. S. Shelkovsky, and V. V. Orlov, *Int. J. Mass Spectrom.* **194**, 49 (2000).
81. M. V. Kosevich, *Probl. Kriobiol*. **2**, 54 (1999) (in Russian).
82. G. B. Pronchev, I. A. Korobeinikova, and A. N. Ermakov, *J. Anal. Chem.* **65**, 940 (2010).
83. L. G. Björn and F. Arnold, *Geophys. Res. Lett.* **8**, 1167 (1981).
84. T. R. Sharp, *Org. Mass Spectrom.* **21**, 793 (1986).
85. G. B. Pronchev, I. A. Korobeinikova, and A. N. Yermakov, *Eur. J. Mass Spectrom.* 8, 131 (2002).
86. I. A. Korobeinikova, G. B. Pronchev, and A. N. Yermakov, *J. Trace Microprobe Tech.* **20**, 105 (2002).
87. I. A. Korobeinikova, G. B. Pronchev, and A. N. Ermakov, *J. Anal. Chem.* **64**, 136 (2009).
88. C. H. Becker, L. E. Jusinski, and L. Moro, *Int. J. Mass Spectrom. Ion Proc.* **95**, R1 (1990).
89. R. W. Nelson, R. M. Thomas, and P. Williams, *Rapid Commun. Mass Spectrom.* **4**, 348 (1990).
90. P. Williams, *Int. J. Mass Spectrom. Ion Proc.* **131**, 335 (1994).
91. S. Berkenkamp, M. Karas, and F. Hillenkamp, *Proc. Natl. Acad. Sci. U. S. A.* **93**, 7003 (1996).
92. M. E. Belov, S. S. Alimpiev, V. V. Mlynski, S. M. Nikiforov, and P. J. Derrick, *Rapid Commun. Mass Spectrom.* **9**, 1431 (1995).
93. P. Kraft, S. Alimpiev, E. Dratz, and J. Sunner, *J. Amer. Soc. Mass Spectrom.* **9**, 912 (1998).
94. M. L. Baltz-Knorr, K. E. Scriver, and R. F. Haglund, *Appl. Surf. Sci*. **197–198**, 11 (2002).
95. C. E. Von Seggern, B. D. Gardner, and R. J. Cotter, *Anal. Chem.* **76**, 5887 (2004).
96. A. Pirkl, J. Soltwisch, F. Draude, and K. Dreisewerd, *Anal. Chem.* **84**, 5669 (2012).
97. L. Witt, A. Pirkl, F. Draude, J. Peter-Katalinić, K. Dreisewerd, and M. Mormann, *Anal. Chem.* 86, 6439 (2014).
98. C. Mihesan, M. Ziskind, B. Chazallon, C. Focsa, and J. L. Destombes, *Appl. Surf. Sci*. **248**, 238 (2005).
99. M. Ziskind, C. Mihesan, N. Lebrun, B. Chazallon, C. Focsa, and J. L. Destombes, *Appl. Phys. A* **79**, 991 (2004).
100. R. Yang and M. S. Gudipati, *J. Chem. Phys.* **140**, 104202 (2014).
101. B. L. Henderson and M. S. Gudipati, *J. Phys. Chem. A* **118**, 5454 (2014).
102. J. I. Berry, S. Sun, Y. Dou, A. Wucher, and N. Winograd, *Anal. Chem.* **75**, 5146 (2003).
103. G. Robichaud, J. A. Barry, and D. C. Muddiman, *J. Am. Soc. Mass Spectrom.* **25**, 319 (2014).
104. A. Tu and D. C. Muddiman, *J. Am. Soc. Mass Spectrom.* **30**, 2380 (2019).

105. N. Ogrinc, P. Saudemont, J. Balog, Y.-M. Robin, J.-P. Gimeno, Q. Pascal, D. Tierny, Z. Takats, M. Salzet, and I. Fournier, *Nat. Protoc.* **14**, 3162 (2019).
106. T. P. Roddy, D. M. Cannon, G. S. Ostrowski, A. G. Ewing, and N. Winograd, *Anal. Chem.* **75**, 4087 (2003).
107. S. Yoon and T. G. Lee, *Nano Converg.* **5**, 24 (2018).
108. W. Okumura, D. Aoki, Y. Matsushita, M. Yoshida, and K. Fukushima, *Sci. Rep.* **7**, 5939 (2017).
109. J. S. Fletcher, N. P. Lockyer, and J. C. Vickerman, *Mass Spectrom. Rev.* **30**, 142 (2011).
110. N. Winograd and A. Bloom, *Methods Mol. Biol.* **1203**, 9 (2015).
111. D. P. P. Andrade, H. M. Boechat-Roberty, R. Martinez, M. G. P. Homem, E. F. da Silveira, and M. L. M. Rocco, *Surf. Sci.* **603**, 1190 (2009).
112. D. P. P. Andrade, M. L. M. Rocco, H. M. Boechat-Roberty, P. Iza, R. Martinez, M. G. P. Homem, and E. F. da Silveira, *J. Electron Spectrosc. Relat. Phenom.* **155**, 124 (2007).
113. A. T. Lebedev, D. M. Mazur, O. V. Polyakova, D. S. Kosyakov, A. Yu Kozhevnikov, T. B. Latkin, Yu. I. Andreeva, and V. B. Artaev, *Environ. Pollut.* **239**, 416 (2018).
114. D. M. Mazur, T. B. Latkin, D. S. Kosyakov, A. Yu. Kozhevnikov, N. V. Ul'yanovskii, A. G. Kirilov, and A. T. Lebedev, *Environ. Pollut.* **265(B)**, 114885 (2020).
115. A. T. Lebedev, D. M. Mazur, V. B. Artaev, and G. Y. Tikhonov, *Environ. Chem. Lett.* **18**, 1753 (2020).
116. D. M. Mazur, M. Harir, P. Schmitt-Kopplin, O. V. Polyakova, and A. T. Lebedev, *Sci. Total Environ.* **557–558**, 12 (2016).
117. S. A. Sandford, M. Nuevo, P. P. Bera, and T. J. Lee, *Chem. Rev.* 120, 4616 (2020).
118. E. Herbst and E. F. van Dishoeck, *Annu. Rev. Astron. Astrophys.* **47**, 427 (2009).
119. P. Caselli and C. Ceccarelli, *Astron. Astrophys. Rev.* **20**, 56 (2012).
120. M. P. Bernstein, S. A. Sandford, and L. J. Allamandola, *Sci. Am.* **281**, 42 (1999).
121. *Laboratory Astrochemistry*: *From Molecules through Nanoparticles to Grains*, S. Schlemmer, T. Giesen, H. Mutschke, and C. Jager (eds.), Wiley-VCH, Weinheim (2015).
122. D. J. Burke and W. A. Brown, *Phys. Chem. Chem. Phys.* **12**, 5947 (2010).
123. J. P. Dworkin, J. S. Gillette, M. P. Bernstein, S. A. Sandford, L. J. Allamandola, J. E. Elsila, D. R. McGlothlin, and R. N. Zare, *Adv. Space Res.* **33**, 67 (2004).
124. D. M. Paardekooper, J.-B. Bossa, K. Isokoski, and H. Linnartz, *Rev. Sci. Instrum.* **85**, 104501 (2014).
125. G. A. Baratta, D. Chaput, H. Cottin, L. Fernandez Cascales, M. E. Palumbo, and G. Strazzulla, *Planet. Space Sci.* **118**, 211 (2015).
126. D. Qasim, M. J. A. Witlox, G. Fedoseev, K.-J. Chuang, T. Banu, S. A. Krasnokutski, S. Ioppolo, J. Kästner, E. F. van Dishoeck, and H. Linnartz, *Rev. Sci. Instrum.* **91**, 054501 (2020).
127. K.-J. Chuang, G. Fedoseev, S. Ioppolo, E. F. van Dishoeck, and H. Linnartz, *Mon. Not. R. Astron. Soc.* **455**, 1702 (2016).
128. F. H. Fied, *J. Phys. Chem.* **86**, 5115 (1982).
129. T. Keough, F. S. Ezra, A. F. Russell, and J. D. Pryne, *Org. Mass. Spectrom.* **22**, 241 (1987).
130. D. A. Mendis, *Annu. Rev. Astron. Astrophys.* **26**, 11 (1988).
131. R. T. Garrod, L. Susanna, W. Widicus, and E. Herbst, *Astrophys. J.* **682**, 283 (2008).

Низькотемпературні вторинно-емісійні мас-спектрометричні дослідження конденсованого оточення біологічно значущих сполук

Marina V. Kosevich, Oleg A. Boryak, Vadim S. Shelkovsky

Підсумовано основні характеристики вторинно-емісійних мас-спектрометричних досліджень конденсованих систем, які містять біологічно значущі сполуки, за умов низьких температур. Проілюстровано можливості розрізнення мас-спектрів твердої та рідкої фаз простих органічних сполук та води як середовища для біомолекул, спостереження за фазовими перетвореннями та нерівноважними процесами. Описано особливості моделі розпилення метастабільних рідин. На основі оцінки цих результатів запропоновано та обговорено ідею стосовно можливого джерела відносно великих кластерів органічних молекул та іонів, які формуються завдяки розпиленню рідкої фази органічного матеріалу, конденсованого на пилових зернах у космічному просторі.

Ключові слова: низькотемпературна вторинно-емісійна мас-спектрометрія, біомолекули, водний лід, спирти, фазові переходи.